Chapter 12
The Importance of Phase-Locking in Nonlinear Modal Interactions

T.L. Hill, A. Cammarano, S.A. Neild, and D.J. Wagg

Abstract In nonlinear systems the constituent linear modes may interact due to internal resonance. In this paper we classify two distinct classes of modal interactions: *phase-locked* interactions, in which there is a specific phase between the interacting modes; and *phase-unlocked* interactions, in which the modes may interact regardless of their phase. This discussion is accompanied by the study of an example structure in which both classes of interaction may be observed. The structure is used to demonstrate the differences between phase-locked and phase-unlocked interactions, both in terms of their individual influence on the response, and in terms of their influence on each other when both classes of interactions are present.

Keywords Backbone curves • Second-order normal forms • Modal analysis • Modal interaction • Phase locking

12.1 Introduction

Nonlinear dynamic behaviour poses a significant challenge in the modelling, design and optimisation of engineering structures. This is due to the complexity of such behaviours, in terms of both the wide variety of phenomena a structure may exhibit, and the number of degrees-of-freedom than may interact to produce these phenomena. One phenomenon that is of particular importance is internal resonance, where coupling within the system is achieved at resonance. This phenomenon is unique to nonlinear interactions, and is seen in a variety of physical structures [1, 2].

Typically, the design of engineering structures requires an understanding of the forced responses. However, when these responses exhibit nonlinear behaviour they can be highly complex to compute and interpret. As a result, many approaches to nonlinear analysis begin by modelling the responses of the underlying conservative systems; for example nonlinear normal modes [3] and backbone curves [4] (note that the study of nonlinear normal modes has also been extended to nonconservative systems [5, 6], and it has been shown that backbone curves can be used to directly interpret the forced responses [7]). Both backbone curves and nonlinear normal modes provide a useful tool for understanding the underlying behaviour of forced responses, and can be used to predict the existence of internal resonances [8, 9]. However, the relative importance of different backbone curves can vary, as the underlying behaviours they describe may not always manifest themselves in the forced responses; for example, if the forcing amplitude is insufficient to reach a backbone curve, the influence of that backbone curve will not be observed [7].

In this paper we investigate the significance of *phase-locking* in backbone curve models. Phase-locking is defined as a condition imposed upon the phase relationship between the underlying linear modes of a system. Although the backbone curves may exhibit a variety of different phase relationships [8], these relationships are typically fixed for all responses represented by the backbone curves. However, as will be shown here, there also exist phase-unlocked backbone curves, where the modes may exhibit *any* phase relationship. To demonstrate this, we consider a pinned-pinned beam that with a geometric nonlinearity, as considered in [10].

Two separate configurations of this beam are considered: one with an additional rotational stiffness at one end, leading to an asymmetry in the beam; and one without any additional rotational stiffness, and hence with a symmetric structure. The backbone curves of this beam are found using the second-order normal form technique [11, 12], and it is shown that the

T.L. Hill (✉) • S.A. Neild
Department of Mechanical Engineering, University of Bristol, Queen's Building, University Walk, Bristol BS8 1TR, UK
e-mail: tom.hill@bristol.ac.uk

A. Cammarano
School of Engineering, University of Glasgow, Glasgow G12 8QQ, UK

D.J. Wagg
Department of Mechanical Engineering, University of Sheffield, Sir Frederick Mappin Building, Mappin Street, Sheffield S1 3JD, UK

G. Kerschen (ed.), *Nonlinear Dynamics, Volume 1*, Conference Proceedings of the Society for Experimental Mechanics Series,
DOI 10.1007/978-3-319-29739-2_12

asymmetric case has phase-locked backbone curves, whilst the symmetric case only has phase-unlocked backbone curves. By examining the forced responses of the beam it is shown that the behaviour described by the phase-locked backbone curves leads to internal resonance in the forced responses, whilst the phase-unlocked backbone curves do not lead to internal resonance. Finally, it is demonstrated that, whilst the phase-unlocked backbone curves do not predict the existence of internal resonance, they do still describe fundamental behaviours of the system when the system is subjected to particular forcing configurations. These observations indicate an important difference between these two classes of behaviour.

12.2 The Second-Order Normal Form Technique

12.2.1 The Example System

In this paper we consider the pinned-pinned beam with an additional rotational stiffness at one end, as shown in Fig. 12.1. Two specific cases are considered here: one in which the additional rotational stiffness, k, is zero (such that the beam is symmetric); and one in which $k = 10\,\mathrm{N\,m\,rad^{-1}}$, such that the beam is asymmetric. In both cases, the beam has dimensions $L = 500\,\mathrm{mm}$, $w = 30\,\mathrm{mm}$ and $h = 1\,\mathrm{mm}$. Additionally, the beam has a density and Young's modulus of $\rho = 7800\,\mathrm{kg\,m^{-3}}$, $E = 200 \times 10^9\,\mathrm{N\,m^{-2}}$ respectively. A similar configuration of a beam has previously discussed in [10], where it is shown that the unforced and undamped behaviour of the beam may be modelled using the first two linear modes, using the equations of motion, written

$$\ddot{q}_1 + \omega_{n1}^2 q_1 + \mu^2 \left(\gamma_{11} q_1^2 + 2\gamma_{12} q_1 q_2 + \gamma_{22} q_2^2\right)\left(\gamma_{11} q_1 + \gamma_{12} q_2\right) = 0\,, \tag{12.1a}$$

$$\ddot{q}_2 + \omega_{n2}^2 q_2 + \mu^2 \left(\gamma_{11} q_1^2 + 2\gamma_{12} q_1 q_2 + \gamma_{22} q_2^2\right)\left(\gamma_{12} q_1 + \gamma_{22} q_2\right) = 0\,, \tag{12.1b}$$

where: q_i represents the displacement of the ith linear mode; ω_{ni} represents ith linear natural frequency; and μ, γ_{11}, γ_{12} and γ_{22} are nonlinear parameters. These expressions may be written in the form

$$\ddot{\mathbf{q}} + \mathbf{\Lambda q} + \mathbf{N}_q\left(\mathbf{q}\right) = 0\,, \tag{12.2}$$

where: $\mathbf{q}$ is a vector of modal displacements, in which the ith element in $\mathbf{q}$ is q_i; $\mathbf{\Lambda}$ is a diagonal matrix whose ith leading diagonal element is the square of the ith linear natural frequency, ω_{ni}^2; and $\mathbf{N}_q$ is a vector of nonlinear terms, written

$$\mathbf{N}_q\left(\mathbf{q}\right) = \begin{pmatrix} \alpha_1 q_1^3 + 3\alpha_2 q_1^2 q_2 + \alpha_3 q_1 q_2^2 + \alpha_4 q_2^3 \\ \alpha_2 q_1^3 + \alpha_3 q_1^2 q_2 + 3\alpha_4 q_1 q_2^2 + \alpha_5 q_2^3 \end{pmatrix}, \tag{12.3}$$

where

$$\begin{aligned} &\alpha_1 = \mu^2\gamma_{11}^2\,, \quad \alpha_2 = \mu^2\gamma_{11}\gamma_{12}\,, \quad \alpha_3 = \mu^2\left(\gamma_{11}\gamma_{22} + 2\gamma_{12}^2\right)\,, \\ &\alpha_4 = \mu^2\gamma_{12}\gamma_{22}\,, \quad \alpha_5 = \mu^2\gamma_{22}^2\,. \end{aligned} \tag{12.4}$$

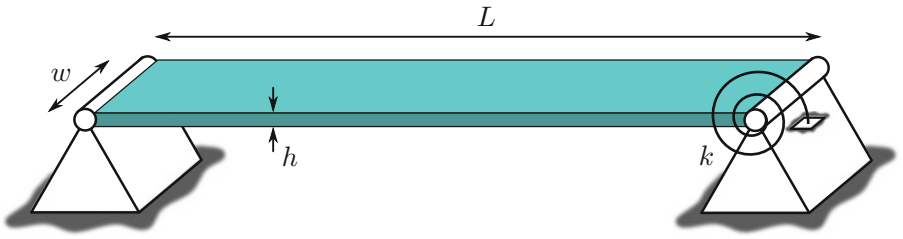

Fig. 12.1 Schematic of a pinned-pinned beam with a rotational constraint at one end

Table 12.1 The linear natural frequencies and nonlinear parameters for the two different configurations of the beam

	ω_{n1}	ω_{n2}	α_1	α_2	α_3	α_4	α_5
	(rad s^{-1})		$(\times 10^{10})$				
Symmetric case ($k = 0$)	57.71	230.83	2.00	0	8.00	0	31.98
Asymmetric case ($k = 10$)	125.91	418.41	8.81	−1.31	34.7	−5.12	133.63

From [10], it is found that, for the two different cases considered here (i.e. when the beam is symmetric, and when the beam is asymmetric) the linear natural frequencies and nonlinear parameters have the values given in Table 12.1. It can be seen that, when the beam is symmetric, i.e. when $k = 0$, then $\alpha_2 = \alpha_4 = 0$.

12.2.2 Applying the Second-Order Normal Form Technique to the Example System

The backbone curves of a system describe the loci of unforced, undamped dynamic responses of a system. In order to find the backbone curves of the example system considered here, we apply the second-order normal form technique to the unforced, undamped equations of motion, Eq. (12.2). This technique is detailed in [11], and it was first demonstrated how the technique may be used to find the backbone curves of nonlinear systems in [4].

The second-order normal form technique typically consists of three steps: the linear modal transform, which transforms the equations of motion from physical into linear modal coordinates; the forcing transform, which removes any non-resonant forcing terms from the equations of motion; and the nonlinear near-identity transform, which removes any non-resonant (i.e. harmonic) terms from the equations of motion. This results in a set of approximate, analytical expressions containing only the resonant components of the motion, which may then be solved using an assumed solution. For the case considered here, the equations of motion, Eq. (12.2), are expressed in terms of the linear modal coordinates and therefore the linear modal transform is not necessary. Additionally, the system is unforced (as we are considering the backbone curves) and hence the forcing transform is also not needed. Thus, in this case, the second-order normal form technique consists only of the nonlinear near-identity transform, applied directly to Eq. (12.2).

The nonlinear near-identity transform involves the substitution $\mathbf{q} = \mathbf{u} + \mathbf{h}$ where $\mathbf{u}$ and $\mathbf{h}$ represent the fundamental and harmonic components of $\mathbf{q}$ respectively. It is assumed that the harmonics are small and, as the nonlinear terms are also assumed to be small, the approximation $\mathbf{N}_q(\mathbf{q}) = \mathbf{N}_q(\mathbf{u})$ is made. Additionally, as non-resonant terms are removed, the fundamental component of the response, $\mathbf{u}$, is sinusoidal, and therefore the ith element of $\mathbf{u}$ may be written

$$u_i = \cos(\omega_{ri} t - \phi_i) , \tag{12.5a}$$

$$= u_{pi} + u_{mi} = \frac{U_i}{2} \mathrm{e}^{+\mathrm{j}(\omega_{ri} t - \phi_i)} + \frac{U_i}{2} \mathrm{e}^{-\mathrm{j}(\omega_{ri} t - \phi_i)} , \tag{12.5b}$$

where U_i, ω_{ri} and ϕ_i are the amplitude, response frequency and phase respectively. Note that the subscripts "p" and "m" in Eq. (12.5b), correspond to the positive and negative, i.e. *plus* and *minus*, signs in the exponents respectively. Now, substituting $\mathbf{q} = \mathbf{u}$ into Eq. (12.3), along with the assumed solutions, Eq. (12.5b), gives

$$\mathbf{N}_q(\mathbf{u}) = \begin{pmatrix} \alpha_1 (u_{p1} + u_{m1})^3 + 3\alpha_2 (u_{p1} + u_{m1})^2 (u_{p2} + u_{m2}) + \\ \alpha_2 (u_{p1} + u_{m1})^3 + \alpha_3 (u_{p1} + u_{m1})^2 (u_{p2} + u_{m2}) + \\ \qquad \alpha_3 (u_{p1} + u_{m1}) (u_{p2} + u_{m2})^2 + \alpha_4 (u_{p2} + u_{m2})^3 \\ \qquad 3\alpha_4 (u_{p1} + u_{m1}) (u_{p2} + u_{m2})^2 + \alpha_5 (u_{p2} + u_{m2})^3 \end{pmatrix} . \tag{12.6}$$

After expanding the terms in Eq. (12.6), $\mathbf{N}_q$ may be written

$$\mathbf{N}_q(\mathbf{u}) = \left[N_q \right] \mathbf{u}^* (\mathbf{u}_p, \mathbf{u}_m) , \tag{12.7}$$

where: $\mathbf{u}^*$ is a vector containing all unique combinations of the variables u_{pi} and u_{mi} (expressed in the vectors $\mathbf{u}_p$ and $\mathbf{u}_m$); and $\left[N_q\right]$ is a matrix of the coefficients corresponding to those variables. As the elements in $\mathbf{u}^*$ are composed only of u_{pi} and u_{mi}, the ℓth element of $\mathbf{u}^*$ may be written

$$u_\ell^* = \prod_{n=1}^{N} u_{pn}^{s_{p,\ell,n}} u_{mn}^{s_{m,\ell,n}}, \tag{12.8}$$

where N is the number of degrees-of-freedom of the system (i.e. $N = 2$ in the case considered here). Using Eq. (12.8), the exponents $s_{p,\ell,n}$ and $s_{m,\ell,n}$ can be found, allowing the matrix $\boldsymbol{\beta}$ to be defined, where element $\{i,\ \ell\}$ of $\boldsymbol{\beta}$ is given by

$$\beta_{i,\ell} = \left[\sum_{n=1}^{N} \left(s_{p,\ell,n} - s_{m,\ell,n}\right) \omega_{rn}\right]^2 - \omega_{ri}^2 . \tag{12.9}$$

It is the matrix $\boldsymbol{\beta}$ which allows us to determine which nonlinear terms are resonant, and thus appear in the resonant equation of motion. However, it can be seen from Eq. (12.9) that $\boldsymbol{\beta}$ is dependent on the fundamental response frequencies, ω_{ri}, and therefore the ratios between these frequencies must be known in order to determine which terms are resonant. Typically, as discussed in [11], the ratios between the response frequencies are chosen based upon the ratios between the linear natural frequencies, i.e. if $\omega_{n1} \approx \omega_{n2}$, then it is assumed that the modes will respond at the same frequency. However, here we wish to investigate how this ratio influences which terms are resonant, and hence it is assumed that the fundamental component of q_2 responds at r times that of q_1, i.e. $\omega_{r2} = r\omega_{r1}$. Substituting this into Eq. (12.9) allows $\boldsymbol{\beta}$ to be defined, for this case, as

$$\beta_{1,\ell} = \left\{\left[s_{p,\ell,1} - s_{m,\ell,1} + r\left(s_{p,\ell,2} - s_{m,\ell,2}\right)\right]^2 - 1\right\} \omega_{r1}^2 , \tag{12.10a}$$

$$\beta_{2,\ell} = \left\{\left[s_{p,\ell,1} - s_{m,\ell,1} + r\left(s_{p,\ell,2} - s_{m,\ell,2}\right)\right]^2 - r^2\right\} \omega_{r1}^2 . \tag{12.10b}$$

Now, Eqs. (12.6)–(12.8) and (12.10) may be used to write $\left[N_q\right]$, $\mathbf{u}^*$ and $\boldsymbol{\beta}$ as

$$\left[N_q\right]^\mathsf{T} = \begin{bmatrix} \alpha_1 & \alpha_2 \\ 3\alpha_1 & 3\alpha_2 \\ 3\alpha_1 & 3\alpha_2 \\ \alpha_1 & \alpha_2 \\ 3\alpha_2 & \alpha_3 \\ 6\alpha_2 & 2\alpha_3 \\ 3\alpha_2 & \alpha_3 \\ 3\alpha_2 & \alpha_3 \\ 6\alpha_2 & 2\alpha_3 \\ 3\alpha_2 & \alpha_3 \\ \alpha_3 & 3\alpha_4 \\ 2\alpha_3 & 6\alpha_4 \\ \alpha_3 & 3\alpha_4 \\ \alpha_3 & 3\alpha_4 \\ 2\alpha_3 & 6\alpha_4 \\ \alpha_3 & 3\alpha_4 \\ \alpha_4 & \alpha_5 \\ 3\alpha_4 & 3\alpha_5 \\ 3\alpha_4 & 3\alpha_5 \\ \alpha_4 & \alpha_5 \end{bmatrix}, \mathbf{u}^* = \begin{bmatrix} u_{p1}^3 \\ u_{p1}^2 u_{m1} \\ u_{p1} u_{m1}^2 \\ u_{m1}^3 \\ u_{p1}^2 u_{p2} \\ u_{p1} u_{m1} u_{p2} \\ u_{m1}^2 u_{p2} \\ u_{p1}^2 u_{m2} \\ u_{p1} u_{m1} u_{m2} \\ u_{m1}^2 u_{m2} \\ u_{p1} u_{p2}^2 \\ u_{p1} u_{p2} u_{m2} \\ u_{p1} u_{m2}^2 \\ u_{m1} u_{p2}^2 \\ u_{m1} u_{p2} u_{m2} \\ u_{m1} u_{m2}^2 \\ u_{p2}^3 \\ u_{p2}^2 u_{m2} \\ u_{p2} u_{m2}^2 \\ u_{m2}^3 \end{bmatrix}, \tag{}$$

$$\boldsymbol{\beta}^{\mathsf{T}} = \omega_{r1}^2 \begin{bmatrix} 8 & 9-r^2 \\ 0 & 1-r^2 \\ 0 & 1-r^2 \\ 8 & 9-r^2 \\ (r+1)(r+3) & 4(1+r) \\ r^2-1 & 0 \\ (r-1)(r-3) & 4(1-r) \\ (r-1)(r-3) & 4(1-r) \\ r^2-1 & 0 \\ (r+1)(r+3) & 4(1+r) \\ 4r(r+1) & (3r+1)(r+1) \\ 0 & 1-r^2 \\ 4r(r-1) & (3r-1)(r-1) \\ 4r(r-1) & (3r-1)(r-1) \\ 0 & 1-r^2 \\ 4r(r+1) & (3r+1)(r+1) \\ 9r^2-1 & 8r^2 \\ r^2-1 & 0 \\ r^2-1 & 0 \\ 9r^2-1 & 8r^2 \end{bmatrix}. \tag{12.11}$$

The resonant equation of motion is written

$$\ddot{\mathbf{u}} + \boldsymbol{\Lambda}\mathbf{u} + \mathbf{N}_u(\mathbf{u}) = 0\,, \tag{12.12}$$

where $\mathbf{N}_u$ is a vector of resonant nonlinear terms, defined using

$$\mathbf{N}_u(\mathbf{u}) = [n_u]\,\mathbf{u}^*\left(\mathbf{u}_p,\, \mathbf{u}_m\right), \tag{12.13}$$

where $[n_u]$ is a matrix of the coefficients of the resonant nonlinear terms. The nonlinear terms represented by $\left[N_q\right]$ are defined as resonant if they correspond to an element in $\boldsymbol{\beta}$ that contains a zero; hence such a term is also represented in $[n_u]$. Conversely, if a term is non-resonant (i.e. it contributes to a harmonic) then the corresponding element in $\boldsymbol{\beta}$ is non-zero, and hence the element in $[n_u]$ must be zero. This is expressed by the relationship defining element $\{i,\, \ell\}$ of $[n_u]$ as

$$[n_u]_{i,\ell} = \begin{cases} \left[N_q\right]_{i,\ell} & \text{if}: \quad \beta_{i,\ell} = 0\,, \\ 0 & \text{if}: \quad \beta_{i,\ell} \neq 0\,. \end{cases} \tag{12.14}$$

Note that, whilst the harmonics are neglected here, they may be computed using the second-order normal form technique—see [13] for further details.

It can be seen from Eq. (12.11) that the terms in $\boldsymbol{\beta}$ may be separated into three categories:

- *Non-resonant*, which are non-zero, regardless of the value of r,
- *Unconditionally-resonant*, which are zero for all values of r,
- *Conditionally-resonant*, which are only zero for specific values of r.

Furthermore, from Eq. (12.11), it can be seen that, for this case, the conditionally-resonant terms become resonant for three different values of r, namely $r = 1/3$, $r = 1$ and $r = 3$. Therefore, using Eqs. (12.11) and (12.14), the matrix of resonant coefficients, $[n_u]$, may be found, from which Eq. (12.13) may be used to write

$$\mathbf{N}_u = \begin{pmatrix} 3\alpha_1 u_{p1} u_{m1} u_1 + 2\alpha_3 u_{p2} u_{m2} u_1 \\ 2\alpha_3 u_{p1} u_{m1} u_2 + 3\alpha_5 u_{p2} u_{m2} u_2 \end{pmatrix} + \delta\left\{r - \frac{1}{3}\right\} \begin{pmatrix} \alpha_4 \left(u_{p2}^3 + u_{m2}^3\right) \\ 3\alpha_4 \left(u_{p1} u_{m2}^2 + u_{p1} u_{m2}^2\right) \end{pmatrix} + \tag{12.15}$$

$$\delta\{r-1\} \begin{pmatrix} 3\alpha_2 \left(2u_{p1} u_{m1} u_2 + u_{p1}^2 u_{m2} + u_{m1}^2 u_{p2}\right) + \alpha_3 \left(u_{m1} u_{p2}^2 + u_{p1} u_{m2}^2\right) + 3\alpha_4 u_{p2} u_{m2} u_2 \\ 3\alpha_4 \left(2u_1 u_{p2} u_{m2} + u_{m1} u_{p2}^2 + u_{p1} u_{m2}^2\right) + \alpha_3 \left(u_{p1}^2 u_{m2} + u_{m1}^2 u_{p2}\right) + 3\alpha_2 u_{p1} u_{m1} u_1 \end{pmatrix} +$$

$$+\delta\{r-3\} \begin{pmatrix} 3\alpha_2 \left(u_{m1}^2 u_{p2} + u_{p1}^2 u_{m2}\right) \\ \alpha_2 \left(u_{p1}^3 + u_{m1}^3\right) \end{pmatrix},$$

where δ represents the Dirac-delta function.

12.3 The Backbone Curves of the Example System

In order to find the backbone curves, we must solve the time-dependent resonant equations of motion, Eq. (12.12), which first requires that the time-dependence is removed from these equations. In [8] it is shown that the ith element of the vector of resonant nonlinear terms, $\mathbf{N}_u$, may be written

$$N_{ui} = N_{ui}^{+} \mathrm{e}^{+\mathrm{j}\omega_{ri} t} + N_{ui}^{-} \mathrm{e}^{-\mathrm{j}\omega_{ri} t}\,, \tag{12.16}$$

therefore, substituting Eqs. (12.5) and (12.16), the resonant equation of motion, Eq. (12.12), for the ith mode may be written

$$\left[\left(\omega_{ni}^2 - \omega_{ri}^2\right) \frac{U_i}{2} \mathrm{e}^{-\mathrm{j}\phi_i} + N_{ui}^{+}\right] \mathrm{e}^{+\mathrm{j}\omega_{ri} t} + \left[\left(\omega_{ni}^2 - \omega_{ri}^2\right) \frac{U_i}{2} \mathrm{e}^{+\mathrm{j}\phi_i} + N_{ui}^{-}\right] \mathrm{e}^{-\mathrm{j}\omega_{ri} t} = 0\,, \tag{12.17}$$

where the contents of the square brackets form a complex conjugates pair. Therefore, the contents of these brackets may each be equated to zero, i.e.

$$\left(\omega_{ni}^2 - \omega_{ri}^2\right) U_i + 2N_{ui}^{+} \mathrm{e}^{+\mathrm{j}\phi_i} = 0\,, \tag{12.18}$$

where it can be seen that Eq. (12.18) is independent of time.

Now, substituting Eq. (12.5) into Eq. (12.15) allows the complex components N_{ui}^{+} to be identified. These may then be substituted into Eq. (12.18) to give

$$4\left(\omega_{n1}^2 - \omega_{r1}^2\right) U_1 + 3\alpha_1 U_1^3 + 2\alpha_3 U_1 U_2^2 + \delta_{1/3}\alpha_4 U_2^3 \mathrm{e}^{+\mathrm{j}\phi_{d1,3}} + \delta_3 3\alpha_2 U_1^2 U_2 \mathrm{e}^{+\mathrm{j}\phi_{d3,1}}$$
$$+\delta_1 \left[3\alpha_2 U_1^2 U_2 \left(2 + \mathrm{e}^{-\mathrm{j}2\phi_{d1,1}}\right) + \alpha_3 U_1 U_2^2 \mathrm{e}^{+\mathrm{j}\phi_{d1,1}} + 3\alpha_4 U_2^3\right] \mathrm{e}^{+\mathrm{j}\phi_{d1,1}} = 0\,, \tag{12.19a}$$

$$4\left(\omega_{n2}^2 - r^2\omega_{r1}^2\right) U_2 + 2\alpha_3 U_1^2 U_2 + 3\alpha_5 U_2^3 + \delta_{1/3} 3\alpha_4 U_1 U_2^2 \mathrm{e}^{-\mathrm{j}\phi_{d1,3}} + \delta_3 \alpha_2 U_1^3 \mathrm{e}^{-\mathrm{j}\phi_{d3,1}}$$
$$+\delta_1 \left[3\alpha_2 U_1^3 + \alpha_3 U_1^2 U_2 \mathrm{e}^{-\mathrm{j}\phi_{d1,1}} + 3\alpha_4 U_1 U_2^2 \left(2 + \mathrm{e}^{+\mathrm{j}2\phi_{d1,1}}\right)\right] \mathrm{e}^{-\mathrm{j}\phi_{d1,1}} = 0\,, \tag{12.19b}$$

where the phase difference, $\phi_{di,j}$, is defined as $\phi_{di,j} = i\phi_1 - j\phi_2$, and the Dirac-delta function is denoted $\delta_k = \delta\{r-k\}$. Note that $\omega_{r2} = r\omega_{r1}$ has been used.

Equation (12.19) demonstrate that some terms are a function of the phase difference between the two modes (where the phase difference is dependent on r). As will be shown in the following sections, such terms enforce a specific phase-relationship for resonant responses described by the backbone curve, known as *phase-locking*. It therefore follows that backbone curves that are described by expressions which are not a function of the phase difference do not have a specific phase-relationship, and the responses they describe may therefore exhibit any phase value between the modes. Furthermore, it can be seen in Eq. (12.19) that the terms which exhibit a phase-dependence are also those that are dependent on r i.e. are conditionally resonant terms, suggesting a relationship between conditional resonance and phase-locking.

12.3.1 The Backbone Curves of the Asymmetric Case

From Table 12.1 it can be seen that, for the asymmetric case, all nonlinear parameters, α_i, are non-zero. Additionally, the ratio between the linear natural frequencies, $\omega_{n1}{:}\omega_{n2}$, is approximately 1:3 . Therefore, it seems likely that a similar ratio will exist between the response frequencies, and hence the case where $r = 3$ is considered. From Eq. (12.19) this leads to

$$4\left(\omega_{n1}^2 - \omega_{r1}^2\right) U_1 + 3\alpha_1 U_1^3 + 2\alpha_3 U_1 U_2^2 + 3\alpha_2 U_1^2 U_2 \mathrm{e}^{+\mathrm{j}\,(3\phi_1 - \phi_2)} = 0\,, \tag{12.20a}$$

$$4\left(\omega_{n2}^2 - 9\omega_{r1}^2\right) U_2 + 2\alpha_3 U_1^2 U_2 + 3\alpha_5 U_2^3 + \alpha_2 U_1^3 \mathrm{e}^{-\mathrm{j}\,(3\phi_1 - \phi_2)} = 0\,. \tag{12.20b}$$

As we are concerned with the phase difference between the modes, we consider the case where both modal amplitudes are non-zero. Therefore, the imaginary components of Eq. (12.20) both lead to $\sin(3\phi_1 - \phi_2) = 0$, which may be satisfied by $3\phi_1 - \phi_2 = 0,\ \pi,\ \ldots$, thus enforcing phase-locking between the modes. The real components of Eq. (12.20) may then be written

$$4\left(\omega_{n1}^2 - \omega_{r1}^2\right) + 3\alpha_1 U_1^2 + 2\alpha_3 U_2^2 + p3\alpha_2 U_1 U_2 = 0\,, \tag{12.21a}$$

$$4\left(\omega_{n2}^2 - 9\omega_{r1}^2\right) U_2 + 2\alpha_3 U_1^2 U_2 + 3\alpha_5 U_2^3 + p\alpha_2 U_1^3 = 0\,, \tag{12.21b}$$

where

$$p = \begin{cases} +1 & \text{when}: \quad 3\phi_1 - \phi_2 = 0\,, \\ -1 & \text{when}: \quad 3\phi_1 - \phi_2 = \pi\,. \end{cases} \tag{12.22}$$

Here, the backbone curves associated with the solutions to the $p = +1$ case (i.e. where the linear modes are in-phase) are denoted S_1^+, and the solutions to the $p = -1$ case (i.e. where the linear modes are in anti-phase) are denoted S_1^-.

The backbone curves S_1^+ and S_1^-, found using Eq. (12.21) are shown in Fig. 12.2, along with the response of the system when subject to forcing in the first linear mode (i.e. the second mode is unforced). A linear, proportional damping model is used for this forcing case, i.e. the damping term in the ith linear equation of motion is $2\zeta\omega_{ni}\dot{q}_i$, where ζ is the modal damping ratio, which is equal for both modes. The forcing applied to the first linear mode is sinusoidal, at amplitude P_1. In the case

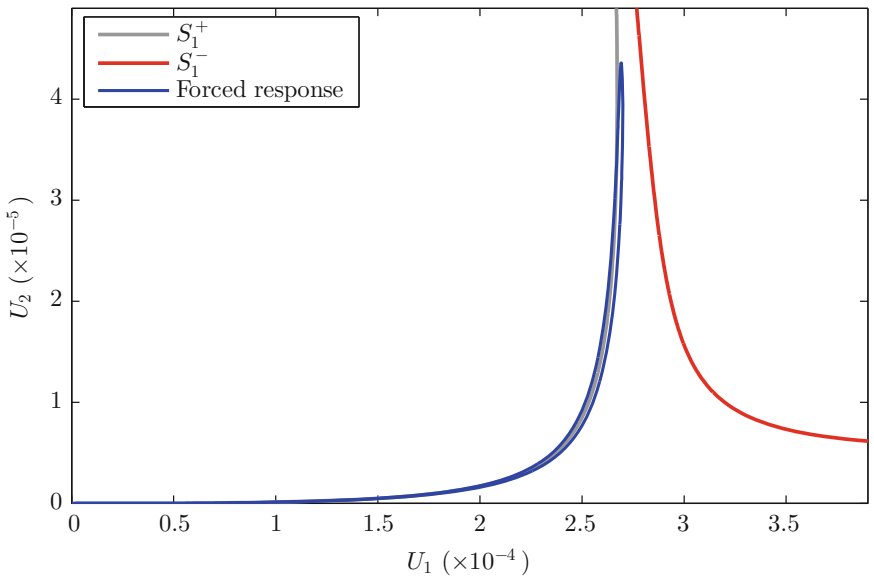

Fig. 12.2 The backbone curves and a forced response of the asymmetric beam. This is shown in the projection of the amplitude of the fundamental component of first linear mode, U_1, against that of the second linear mode, U_2. The backbone curves S_1^+ and S_1^- are represented by a *grey line* and a *red line* respectively, whilst the forced response is represented by a *blue line*

shown in Fig. 12.2, the modal damping ratio is $\zeta = 0.1\,\%$, and the forcing amplitude is $P_1 = 0.0175$. These forced responses have been computed using the numerical continuation software AUTO-07p [14].

Figure 12.2 shows that, whilst the forcing is applied directly to the first linear mode, the second mode also exhibits a response, due to internal resonance. Furthermore it can be seen that the forced response branch closely follows the backbone curves; although some deviation can be seen, due to both the approximate nature of the analytical descriptions of the backbone curves, and due to the internal energy transfer required to balance the energy lost through damping, as discussed in [7].

12.3.2 The Backbone Curves of the Symmetric Case

We now consider the symmetric case, where the rotational stiffness at the end of the beam, k, is zero. From Table 12.1, the nonlinear parameters α_2 and α_4 are zero; hence Eq. (12.19) are simplified to

$$4\left(\omega_{n1}^2 - \omega_{r1}^2\right) U_1 + 3\alpha_1 U_1^3 + 2\alpha_3 U_1 U_2^2 + \delta_1 \alpha_3 U_1 U_2^2 \mathrm{e}^{-\mathrm{j}2\left(\phi_1 - \phi_2\right)} = 0\,, \tag{12.23a}$$

$$4\left(\omega_{n2}^2 - r^2\omega_{r1}^2\right) U_2 + 2\alpha_3 U_1^2 U_2 + 3\alpha_5 U_2^3 + \delta_1 \alpha_3 U_1^2 U_2 \mathrm{e}^{-\mathrm{j}2\left(\phi_1 - \phi_2\right)} = 0\,. \tag{12.23b}$$

Equation (12.23) show that the phase-locking only occurs in the symmetric system when $r = 1$; however, it is found that substituting $r = 1$ into Eq. (12.23) does not lead to any valid solutions. This suggests that phase-locking is not possible in the symmetric case.

In [10], a similar case is also discussed (although the phase is not considered) and it is assumed that, as the ratio between the linear natural frequencies is close to 1:3, the response frequencies will also exhibit a 1:3 ratio. Therefore, substituting $r = 3$ into Eq. (12.23) gives

$$\left[4\left(\omega_{n1}^2 - \omega_{r1}^2\right) + 3\alpha_1 U_1^2 + 2\alpha_3 U_2^2\right] U_1 = 0\,, \tag{12.24a}$$

$$\left[4\left(\omega_{n2}^2 - 9\omega_{r1}^2\right) + 2\alpha_3 U_1^2 + 3\alpha_5 U_2^2\right] U_2 = 0\,. \tag{12.24b}$$

It can be seen from Eq. (12.24) that two single-mode solutions exist: one in which $U_2 = 0$, denoted S_1; and another in which $U_1 = 0$, denoted S_2. Additionally a mixed-mode solution exists, in which $U_1 \neq 0$ and $U_2 \neq 0$, denoted S_3. However, unlike the mixed-mode solutions in the asymmetric case, this has no phase-locking. Therefore, whilst the S_1^+ and S_1^- backbone curves of the asymmetric case have specific phase relationships, it appears that the mixed-mode backbone curves described by Eq. (12.24) may exist for any phase difference between the modes.

The backbone curves S_1 and S_3 are shown in Fig. 12.3, along with the response of the system when forced in the shape of the first linear mode. As with Fig. 12.2, a linear proportional damping model is used; however the modal damping ratio is higher, at $\zeta = 0.5\,\%$. The first linear mode is subjected to a sinusoidal forcing at amplitude $P_1 = 0.035$, whilst the second mode is unforced. As in the previous example, this forced response has been computed using numerical continuation, whilst the backbone curves have been calculated using the analytical expressions Eq. (12.24).

Figure 12.3 clearly shows that the forced response follows the backbone curve S_1 (which is composed of only the first mode). The S_3 backbone curve does not appear to influence this forced branch and inspection of the U_2 component reveals that there is no response in the second mode. Additionally, stability analysis of the forced branch reveals that there is no loss of stability in the region surrounding the bifurcation from S_1 onto S_3. Typically, such bifurcations are associated with internally resonant behaviour [15] and lead to bifurcations in the forced branches, along with a loss of stability. Therefore, the backbone curve bifurcation, seen in Fig. 12.3, appears to reveal a special case. This highlights an important difference between the behaviour of phase-locked backbone curves, such as those shown in Fig. 12.2 which exhibit internal resonance, and phase-unlocked backbone curves, such as S_3 in Fig. 12.3 which does not lead to internal resonance.

Although phase-unlocked backbone curves do not lead to internally-resonant behaviour, they may still be used to represent fundamental behaviours in the forced responses. This is demonstrated in Fig. 12.4, where the symmetric case shown in Fig. 12.3 (i.e. with modal damping ratio $\zeta = 0.5\,\%$ and a forcing amplitude $P_1 = 0.035$ applied to first mode) is reconsidered. However, in this case, a forcing is also applied to the second linear mode, with amplitude P_2, and with a frequency that is three times that of the first. As internal resonance is not exhibited by this system, this forcing configuration enforces a 1:3 response ratio, as assumed in the derivation of the backbone curve expressions.

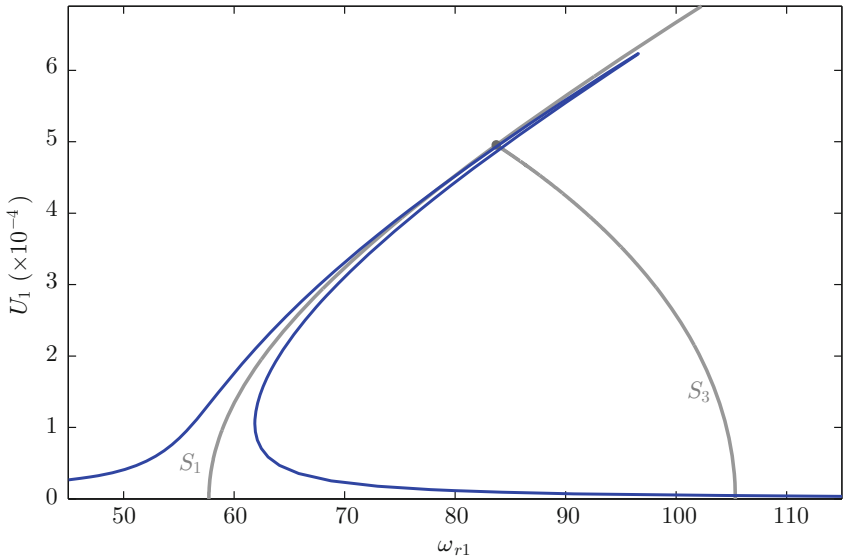

Fig. 12.3 The backbone curves S_1 and S_3, along with a forced response curve of the symmetric beam. This is shown in the projection of the fundamental response frequency of the first linear mode, ω_{r1}, against the fundamental response amplitude of the first linear mode, U_1. Note that it is assumed that ω_{r1} is equal to the forcing frequency. The backbone curves S_1 and S_3 are represented by *grey lines*, and a *grey dot* shows the bifurcation between these two backbone curves. The forced response curve is represented by a *blue line*

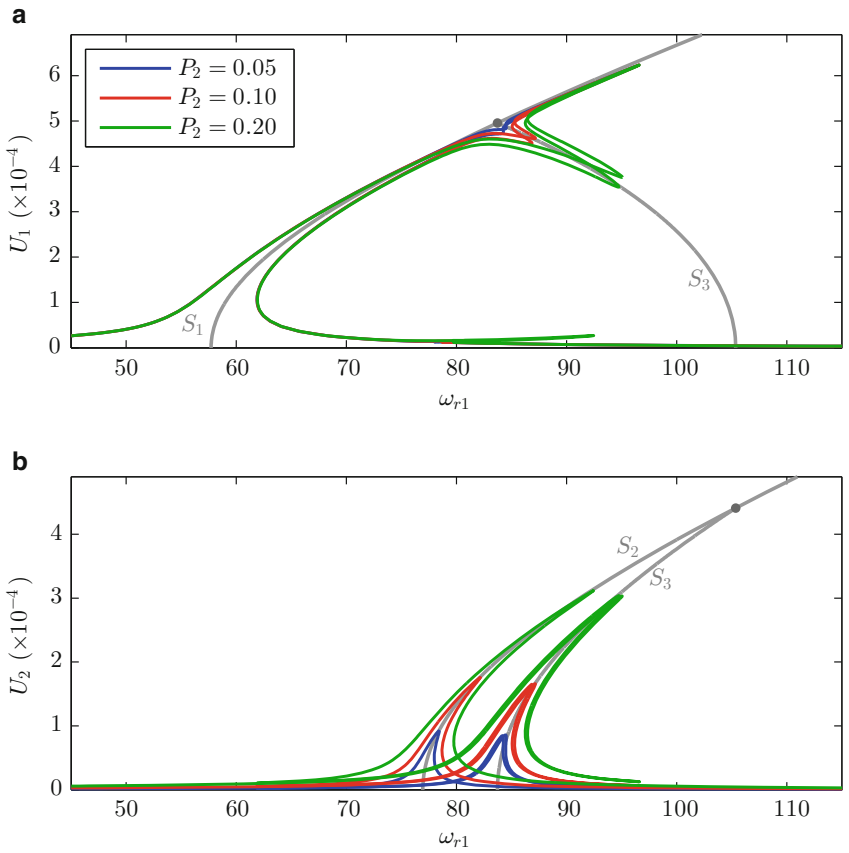

Fig. 12.4 The backbone curves and forced response curves of the symmetric beam when subjected to first and second linear modal forcing. The forcing applied to the second mode is at three times the frequency of the first, and three different forcing amplitudes are used—as shown in the legend in panel **(a)**. Panel **(a)** is shown in the projection of the fundamental response frequency of the first linear mode, ω_{r1}, against the fundamental response amplitude of the first linear mode, U_1, whilst panel **(b)** is shown in the projection of ω_{r1} against U_2. The backbone curves are represented by *grey lines*, and a *grey dot* shows the bifurcation between these two backbone curves

Figure 12.4 shows that, when a 1:3 response ratio is enforced via external forcing, the forced response branches follow the phase-unlocked backbone curve. It has also been confirmed that, as these backbone curves represent responses that may exhibit any phase between the modes, altering the phase between the external forcing does not lead to any significant changes in the forced responses. This demonstrates that such backbone curves represent fundamental underlying behaviours; however, they do not appear to predict internal resonance. As such, it appears that external forcing, or interactions with other modes, is required for the behaviour represented by phase-unlocked backbone curves to manifest.

12.4 Conclusions

In this paper we have demonstrated the difference between phase-locked and phase-unlocked backbone curves. It has been seen that a symmetric beam with nonlinear behaviour, does not have any phase-locked backbone curves. Therefore, the backbone curve of this system describing the 1:3 resonant interaction between the modes, previously discussed in [10], does not exhibit phase-locking. It has been demonstrated that this backbone curve does not lead to internal resonance when the system is forced in only one mode. This is compared to the phase-locked backbone curves of the asymmetric case, where both modes exhibit a response when only one mode is directly forced. This suggests phase-unlocked backbone curves do not describe internally-resonant behaviour, indicating an important difference between these two classes of backbone curves.

It has also been demonstrated that the presence of phase-locking terms may be predicted if the general form of the backbone curves is derived, without the need to assume a specific ratio between the response frequencies. This enables the prediction of those ratios that will lead to phase-locked backbone curves, and those that will not. This feature of the second-order normal form technique represents a significant advantage when compared to analytical techniques that require the response frequency ratio to be selected before such information is known.

References

1. Rao, G.V., Iyengar, R.: Internal resonance and non-linear response of a cable under periodic excitation. J. Sound Vib. **149**(1), 25–41 (1991)
2. Lewandowski, R.: On beams membranes and plates vibration backbone curves in cases of internal resonance. Meccanica **31**(3), 323–346 (1996)
3. Kerschen, G., Peeters, M., Golinval, J.C., Vakakis, A.F.: Nonlinear normal modes, part I: a useful framework for the structural dynamicist. Mech. Syst. Signal Process. **23**(1), 170–194 (2009). Special Issue: Non-linear Structural Dynamics
4. Cammarano, A., Hill, T.L., Neild, S.A., Wagg, D.J.: Bifurcations of backbone curves for systems of coupled nonlinear two mass oscillator. Nonlinear Dyn. **77**(1–2), 311–320 (2014)
5. Shaw, S.W., Pierre, C.: Non-linear normal modes and invariant manifolds. J. Sound Vib. **150**(1), 170–173 (1991)
6. Renson, L., Kerschen, G.: Nonlinear normal modes of nonconservative systems. In: Proceedings of the SEM IMAC XXXI Conference, February 2013
7. Hill, T.L., Cammarano, A., Neild, S.A., Wagg, D.J.: Interpreting the forced responses of a two-degree-of-freedom nonlinear oscillator using backbone curves. J. Sound Vib. **349**, 276–288 (2015)
8. Hill, T.L., Cammarano, A., Neild, S.A., Wagg, D.J.: Out-of-unison resonance in weakly nonlinear coupled oscillators. Proc. R. Soc. Lond. A: Math. Phys. Eng. Sci. **471**(2173) (2014)
9. Jiang, D., Pierre, C., Shaw, S.W.: The construction of non-linear normal modes for systems with internal resonance. Int. J. Non-Linear Mech. **40**(5), 729–746 (2005)
10. Lewandowski, R.: Solutions with bifurcation points for free vibration of beams: an analytical approach. J. Sound Vib. **177**(2), 239–249 (1994)
11. Neild, S.A., Wagg, D.J.: Applying the method of normal forms to second-order nonlinear vibration problems. Proc. R. Soc. A: Math. Phys. Eng. Sci. **467**, 1141–1163 (2011)
12. Wagg, D.J., Neild, S.A.: Approximate methods for analysing nonlinear vibrations. In: Nonlinear Vibration with Control. Solid Mechanics and Its Applications, vol. 218, pp. 145–209. Springer International Publishing, Cham (2015)
13. Neild, S.A., Champneys, A.R. , Wagg, D.J., Hill, T.L., Cammarano, A.: The use of normal forms for analysing nonlinear mechanical vibrations. Philos. Trans. R. Soc. Lond. A: Math. Phys. Eng. Sci. **373**(2051) (2015)
14. Doedel, E.J., with major contributions from A. R. Champneys, Fairgrieve, T.F., Kuznetsov, Y.A., Dercole, F., Oldeman, B.E., Paffenroth, R.C., Sandstede, B., Wang, X.J., Zhang, C.: AUTO-07P: Continuation and Bifurcation Software for Ordinary Differential Equations. Concordia University, Montreal (2008). Available at: http://cmvl.cs.concordia.ca/
15. Hill, T.L., Cammarano, A., Neild, S.A., Wagg, D.J. Relating backbone curves to the forced responses of nonlinear systems. In: Kerschen, G.(ed.) Nonlinear Dynamics, Volume 1, Conference Proceedings of the Society for Experimental Mechanics Series, pp. 113–122. Springer International Publishing, Cham (2016)